Journal of Virology

Virology | Full-Length Text

Inhibition of human adenovirus replication by TRIM35-mediated degradation of E1A

Nan Sun,[1,2,3] Jikai Zhang,[1] Chen Zhang,[1] Tan Xie,[1] Zeyu Zhang,[1] Xueyan Wang,[1] Wanjing Li,[1] Yi Zhang,[1] Zhaokai Chen,[1] Junnian Zheng,[2,3] Lin Fang,[1,2,3] Gang Wang[1,2,3]

AUTHOR AFFILIATIONS See affiliation list on p. 17.

ABSTRACT Human adenovirus (HAdV) is ubiquitous in the human population, constituting a significant burden of global respiratory diseases. Children and individuals with low immunity are at risk of developing severe infections without approved antiviral treatment for HAdV. Our study demonstrated that TRIM35 inhibited HAdV-C5 early gene transcription, early protein expression, genome replication, and infectious virus progeny production. Furthermore, TRIM35 was found to inhibit HAdV replication by attenuating E1A expression. Mechanistically, TRIM35 interacts with and degrades E1A by promoting its K48-linked ubiquitination. Additionally, K253 and K285 are the key sites necessary for TRIM35 degradation. Moreover, an oncolytic adenovirus carrying shTRIM35 was constructed and observed to exhibit improved oncolysis *in vivo*, providing new ideas for clinical tumor treatment. Our results expand the broad antiviral activity of TRIM35 and mechanically support its application as a HAdV replication inhibitor.

IMPORTANCE E1A is an essential human adenovirus (HAdV) protein responsible for the early replication of adenovirus while interacting with multiple host proteins. Understanding the interaction between HAdV E1A and TRIM35 helps identify effective antiviral therapeutic targets. The viral E1A protein is a crucial activator and regulator of viral transcription during the early infection stages. We first reported that TRIM35 interacts with E1A to resist adenovirus infection. Our study demonstrated that TRIM35 targets E1A to resist adenovirus, indicating the applicability of targeting virus-dependent host factors as a suitable antiviral strategy.

KEYWORDS human adenoviruses (HAdV), virus–host interactions, antiviral, TRIM35, E1A, ubiquitination

Human adenovirus (HAdV) is widespread across the population and is a significant burden of respiratory diseases worldwide (1). Diseases due to HAdV vary based on the virus serotype involved, but respiratory infections are common and may cause bronchitis or pneumonia (2, 3). These minor infections are not counted and reported, leading to underrated infection and prevalence of HAdV (4). Furthermore, an adenovirus infection can cause severe diseases. These include disseminated infection, neurological complications, and death in children, the elderly, and immunocompromised individuals (4, 5).

Usually, HAdV must reprogram the intracellular environment to allow the viral genome to replicate in the infected cells once infected (6). During infection, the virus replicates using the host protein interaction network. This either facilitates the virus to hijack host molecular elements and complete its life cycle or counteract the host immune defense for virus removal (7). Once the viral genome enters the nucleus, adenoviral E1A is expressed as the first early gene (8). The E1A gene encodes E1A, a small protein with 289 residues (R) in the HAdV-C5 subtype. The pre-messenger RNA of

Editor Lawrence Banks, International Centre for Genetic Engineering and Biotechnology, Trieste, Italy

Address correspondence to Gang Wang, wangg@xzhmu.edu.cn, Lin Fang, fanglinzhqf@163.com, or Junnian Zheng, jnzheng@xzhmu.edu.cn.

Nan Sun and Jikai Zhang contributed equally to this work. Author order was determined by drawing straws.

The authors declare no conflict of interest.

See the funding table on p. 17.

Received 13 May 2023
Accepted 3 July 2023
Published 14 August 2023

the E1A gene encodes five differentially expressed splice variants during viral infection. E1A is also a significant transactivator of viral early gene expression and a coregulator of many cellular genes (9). The function of E1A is performed mainly by various protein–protein interactions between E1A and host factors (8). Therefore, studying the interaction between E1A and new host factors will help discover novel viral regulatory mechanisms.

Ubiquitination is a common post-translational modification in cells, strongly affecting the structure, localization, function, and stability of the targeted protein across various cellular processes (10, 11). Viral pathogen-associated molecular patterns (PAMPs) and other viral molecules could be targeted by the host ubiquitin system (12, 13). On the other hand, certain viruses have evolved to manipulate the cellular ubiquitination machinery during replication, such as HAdVs (14).

The tripartite motif (TRIMs) family proteins are a class of E3 ubiquitin ligase consisting of the RING-finger domain, B-box domain, Coiled-coil domain, and C-terminal domain (15). TRIMs are involved in the ubiquitination-mediated degradation of various proteins, such as viral proteins (15–17). For instance, TRIM32 can degrade PB1 by ubiquitination, limiting influenza virus infection (18). TRIM69 limits the dengue virus replication by ubiquitinating viral NS3 (19). TRIM22 and TRIM41 exert antiviral activity by degrading viral nucleoprotein and inhibiting influenza A virus infection (20, 21). TRIM35 plays an oncogene role in hepatocellular carcinoma and erythroleukemia (22), with unknown roles during virus infection.

Our previous research has indicated that TRIM35 positively regulated RIG-I-mediated innate immune pathways to inhibit the replication of the influenza A virus (23). However, the role of TRIM35 in HAdV infection remains unclear. This study identified the physical interaction between TRIM35 and E1A. Moreover, overexpression of TRIM35 inhibits HAdV infection, whereas its knockdown increases the susceptibility of the hosts to viral infection. TRIM35 can degrade E1A protein as a ubiquitin E3 ligase through ubiquitination. Our study expands the systematic understanding of TRIM35, suggesting that TRIM35 could be a new host restriction factor in HAdV infection. Consequently, targeting virus-dependent host factors might emerge as a viable antiviral strategy. In addition, given the regulation of TRIM35 on adenovirus replication, we engineered an oncolytic adenovirus (OAV) carrying shTRIM35. Moreover, its more substantial antitumor effect was verified *in vivo*, providing novel ideas for clinical tumor research and therapeutics.

RESULTS

TRIM35 inhibits HAdV replication

Based on our mass spectrometry analysis and virus infection results (Fig. S2; Table S3), we hypothesize that TRIM35 modulates HAdV infection. We assessed the biological effects of TRIM35 overexpression on HAdV infection to investigate the role of TRIM35-E1A interaction in the viral life cycle. First, retrovirus encoding TRIM35 was transduced into A549 cells to establish TRIM35 overexpression stable cell lines and control cell lines with empty retrovirus (24). TRIM35 protein expression was elevated in TRIM35-overexpressing cells than in control cells (Fig. 1A). After infecting control and TRIM35-overexpressing A549 cells with HAdV-C5 at a multiplicity of infection (MOI) of 5 or 20, TRIM35 overexpression negatively affected the virus growth (Fig. 1B). The growth decreased about 10-fold at 24 h with an MOI of 5 with lesser effects at other time points or MOI of 20. No significant effect on cell viability was observed during TRIM35 overexpression with CCK-8 assay (Fig. 1C). HAdV-C5-GFP virus (HAdV-C5-GFP) infected the control and TRIM35-overexpressing A549 cells separately. The results indicated that the number of infected cells decreased, with TRIM35-overexpression inhibiting HAdV-C5 replication (Fig. 1D). TRIM35 in A549 cells was knockdown using small interfering RNA (siRNA) to determine the effect of TRIM35 deletion on viral growth (Fig. 1E). TRIM35-knockdown cells were infected with HAdV-C5 at an MOI of 5 or 20 and virus titers were determined after 24 or 48 h of infection. After TRIM35 depletion, the virus growth was upregulated by 10-fold at the 24 h time point with an MOI of 5 (Fig. 1F). Furthermore, the CCK-8 assay revealed that TRIM35 knockdown had no significant effect on cell viability (Fig. 1G).

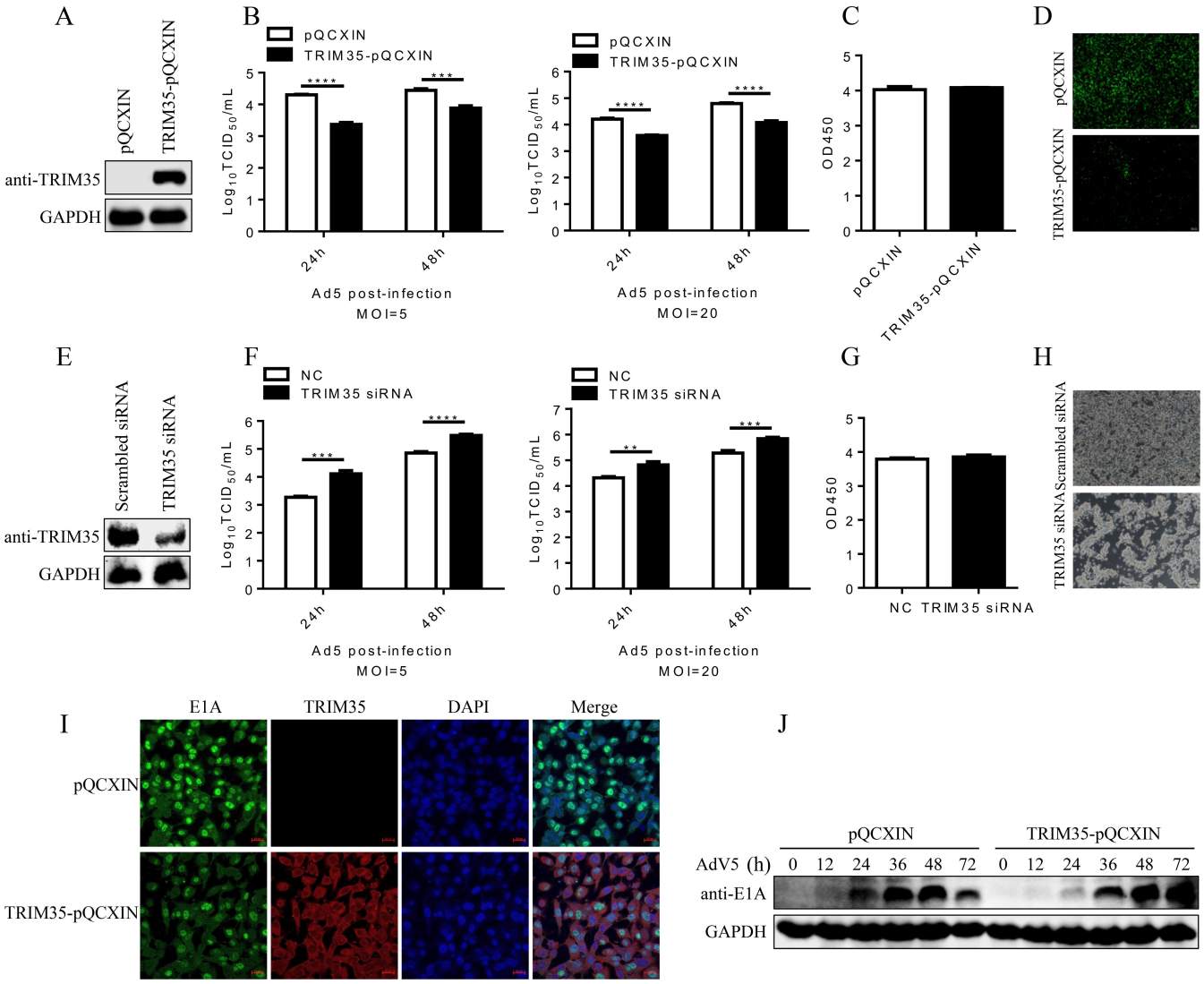

FIG 1 TRIM35 overexpression inhibits HAdV-C5 infection. (A) An A549 cell line stably overexpressing TRIM35 was developed. The western blot confirmed that TRIM35 was overexpressed compared with the empty retrovirus transduced A549 control cell line. (B) Virus replication in TRIM35 overexpressed A549 cells. TRIM35 overexpression or control A549 cells were infected with HAdV-C5 at an MOI of 5 or 20, respectively. The supernatant was collected at specified time points, and the virus titer was determined using TCID50 assays on HEK293 cells. ***, $P < 0.001$; ****, $P < 0.0001$. (C) Measurement of cell viability of overexpressing TRIM35 in A549 cells using CCK-8 assay. The data are expressed as mean ± standard deviation (SD) of three transfections. (D) Virus-infected cells were visualized using fluorescence microscopy. Scale bars, 200 µm. (E) Knockdown of TRIM35 expression in A549 cells using siRNA. After transfecting the A549 cells with TRIM35-targeted or control siRNA for 48 h, we collected the whole cell lysate and subjected it to western blot analysis with rabbit anti-TRIM35. (F) Virus replication in A549 cells treated with siRNA. SiRNA was transfected into cells and HAdV-C5 infected cells with an MOI of 5 or 20. The supernatant was collected at specified time points, and the infectious virus was titrated with TCID50 assays on HEK293 cells. **, $P < 0.01$; ***, $P < 0.001$; ****, $P < 0.0001$. (G) The effect of siRNA-treated TRIM35 on A549 cell viability was detected using CCK-8 assay. The data are expressed as mean ± standard deviation (SD) of three transfections. (H) Virus-infected cells with an MOI of 5 were visualized using brightfield microscopy at 36 h post-infection. Scale bars, 100 µm. (I) IFA of E1A protein expression. HAdV-C5 infected cell lines stably overexpressed TRIM35 or control A549 cells with an MOI of 20 for 12 h, then fixed and stained using anti-E1A antibody. (J) E1A expression in virus-infected cells was detected. The HAdV-C5 virus infected TRIM35 overexpression or control A549 cells with an MOI of 10. The whole cell lysate was collected at specified time points and detected using western blotting with mouse anti-E1A monoclonal antibody. At least three independent experiments were conducted.

Besides, we observed a more severe cytopathic effect induced by HAdV-C5 infection with an MOI of 5 at 36 h in cells treated with TRIM35-specific siRNA than in scrambled siRNA (Fig. 1H). These findings indicate that the knockdown of TRIM35 positively affected virus growth.

HAdV-C5 infected TRIM35 overexpression and empty retrovirus transduced A549 cells with an MOI of 20 to understand E1A distribution during the viral life cycle. Fewer E1A proteins accumulated in the nucleus in TRIM35-overexpressing A549 cells than in control A549 cells at 12 h post-infection (Fig. 1I). The newly synthesized E1A is imported into the nucleus from the cytoplasm, inducing expression of viral gene expression and the completion of the viral replicative cycle (14, 25). In another experiment, E1A expression was detected at 0–72 h after HAdV-C5 infection (Fig. 1J). The observed difference first appeared after 12 h of infection and continued until 72 h. Viral E1A expression was high at 12 h after infection and lasted until 48 h in control A549 cells. However, in TRIM35-overexpressing A549 cells, lesser E1A was detected at 24 h after infection and more at 48 h. Therefore, stable TRIM35 overexpression significantly inhibits E1A expression and virus replication. These results suggest that TRIM35 may be a host restriction factor affecting viral replication and progeny production.

TRIM35 inhibits the transcription of HAdV-C5 genes

Immunofluorescence staining and western blot showed that TRIM35 could inhibit E1A expression during HAdV-C5 infection. Therefore, we detected whether the transcription and genome replication of the HAdV-C5 virus could be inhibited using TRIM35. TRIM35 overexpression cell lines or control A549 cell lines were infected with HAdV-C5. The HAdV-C5 transcripts of E1A, DBP, and Hexon were detected using qPCR. Compared to control cells, E1A, DBP, and Hexon levels were significantly decreased in TRIM35-overexpressing cells at 24 h or 48 h post-infection (Fig. 2A through C). Real-time PCR demonstrated that the TRIM35-overexpressing cell line has a higher TRIM35 expression than the control cell line (Fig. 2D).

We further used siRNA to silence TRIM35 and identified its effect on HAdV-C5 transcription. A549 cells treated with siRNA targeting TRIM35 or control siRNA were infected with the HAdV-C5 virus. Then the E1A, DBP, and Hexon transcripts of HAdV-C5 were detected using qPCR. E1A, DBP, and Hexon levels were significantly elevated in TRIM35-specific siRNA-treated cells (Fig. 2E through G). Meanwhile, real-time PCR confirmed that A549 cells treated with siRNA targeting TRIM35 showed a much lower TRIM35 expression than that in control siRNA-treated A549 cells (Fig. 2H). These results indicate that TRIM35 overexpression inhibits viral genome replication and gene expression.

E1A interacts with TRIM35

As it was unclear if TRIM35 was associated with E1A, we first tested whether they interacted by cotransfecting HEK293 cells with E1A from HAdV-C5 and V5-tagged TRIM35. The interaction between TRIM35 and full-length E1A protein was established with immunoprecipitation (Fig. 3A). Furthermore, E1A was associated with endogenous TRIM35 during normal infection (Fig. 3B). We used V5 tag protein fusions of TRIM35 fragments (DelR, DelB, RBD, and RBCD) (Fig. 3C) and performed coimmunoprecipitation experiments on cotransfected cells to map the interaction region (23). Coimmunoprecipitation experiments revealed that DelR and DelB had negligible effects on TRIM35 and E1A interactions. However, the absence of SPRY (RBD or RBCD) eliminated the interaction, suggesting that the C-terminal SPRY domain is required. Therefore, the PRY/SPRY domain of TRIM35 is essential for E1A interaction (Fig. 3D), which is sufficient to interact with E1A (Fig. 3E). GST pull-down assay also established the interaction of TRIM35-E1A. GST-TRIM35 can pull down E1A but not GST alone (Fig. 3F). Thus, E1A interacts directly with TRIM35. We explored whether E1A and TRIM35 are colocalized in cells. Subsequently, confocal microscopy validated that the two proteins mainly colocalized in the cytoplasm during adenovirus infection (Fig. 3G). In summary, TRIM35 interacts with E1A via the C-terminal region.

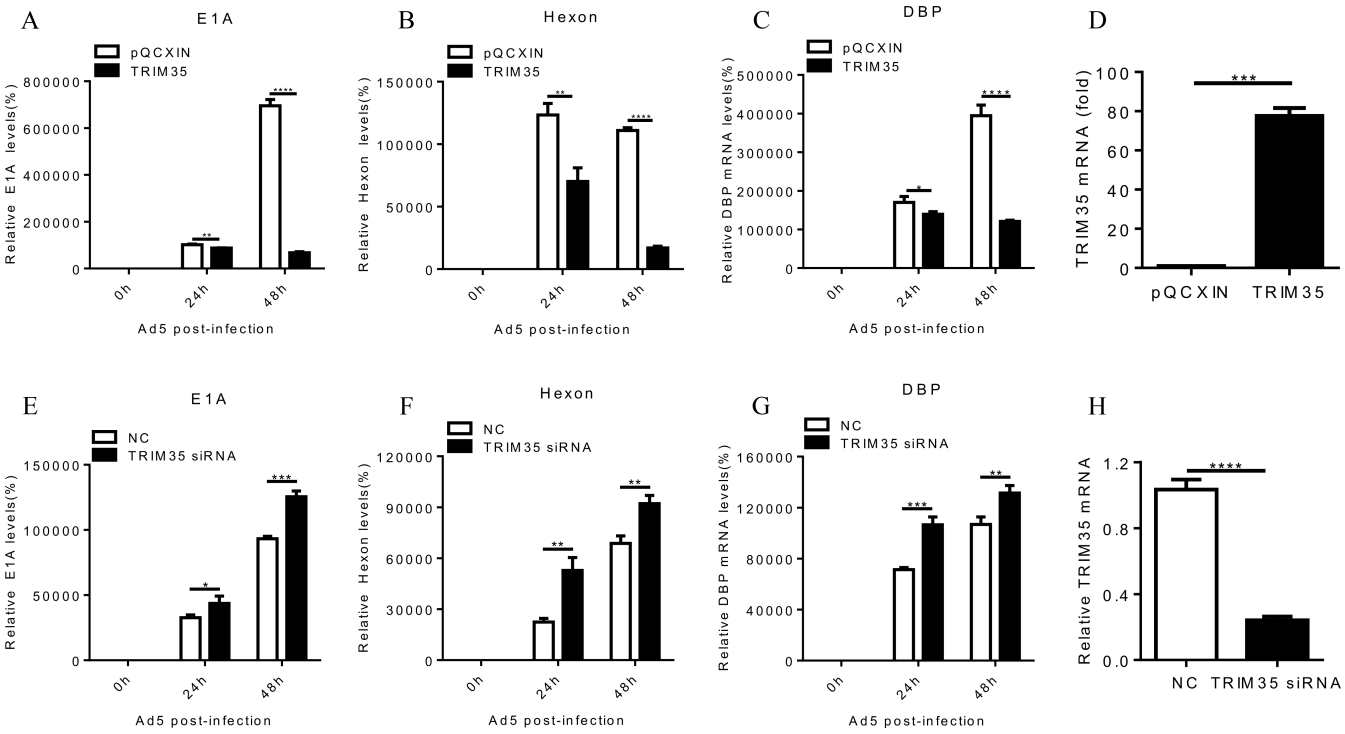

FIG 2 TRIM35 inhibits HAdV-C5 transcription and replication. (A through C) HAdV-C5 infected TRIM35 overexpression or control A549 cells with an MOI of 20. Whole cells were collected at specified time points. RT-qPCR was used to analyze the RNA levels of E1A, DBP, and Hexon transcripts. The represented results are means and SD values from three experiments normalized to acquire for GAPDH. *, $P < 0.05$; **, $P < 0.01$; ****, $P < 0.0001$. (D) Quantitative reverse transcription PCR (RT-qPCR) confirmed the stable overexpression of TRIM35. ***, $P < 0.001$. (E through G) A549 cells were transfected with siRNA targeting TRIM35 or control siRNA for 36 h and infected with HAdV-C5 at an MOI of 20. Subsequently, the whole cells were collected at specified time points, and RT-qPCR analysis was performed using specific primers for E1A, DBP, and Hexon transcripts. The represented results are means and SD values from three experiments normalized to GAPDH results. *, $P < 0.05$; **, $P < 0.01$; ***, $P < 0.001$. (H) Quantitative RT-qPCR confirmed the siRNA knockdown of TRIM35 in A549 cells. ****, $P < 0.0001$. At least three independent experiments were conducted.

TRIM35 promotes Lys48-linked polyubiquitination of E1A

To explore the role of TRIM35 in E1A protein, the wild-type (WT) TRIM35 was transfected into HEK293T cells and infected HAdV-C5. WT TRIM35 decreased E1A protein expression during HAdV-C5 infection (Fig. 4A), indicating that TRIM35 promotes E1A destabilization (26). TRIM proteins utilize their ubiquitin E3 ligase activity to mediate target protein degradation (17, 27, 28). Therefore, we explored whether TRIM35 could degrade HAdV-C5 E1A. Elevated TRIM35 reduced HAdV-C5 E1A protein levels in a dose-dependent manner (Fig. 4B). Western blot analysis revealed that TRIM35 overexpression led to decreased E1A expression (Fig. 4C). HEK293T cells were cotransfected with HAdV-C5-derived E1A and V5-tagged TRIM35 to assess the role of TRIM35 in E1A degradation. Then, they were treated with a protein synthesis inhibitor (cycloheximide) for 2, 4, or 6 h, respectively. Cell lysates were collected and detected using quantitative western blotting. The presence of TRIM35 destabilizes E1A expression (Fig. 4D and E). To determine the role of TRIM35 in E1A degradation, HEK293T cells were transfected with E1A, together with TRIM35 or vector for 24 h and treated with protease inhibitor MG132 for 12 h. Western blot analysis indicated that MG132 prevented the TRIM35-mediated E1A degradation (Fig. 4F).

TRIM35 has E3 ligase activity, suggesting it may ubiquitinate E1A (17, 29). First, we constructed an HA-Ub mutant (K0), and then arginine (R) replaced the lysine (K) residues in K0 (10, 12, 28). Furthermore, the single lysine residues mutants (K6, K11, K27, K29, K33, K48, or K63) were constructed to determine the type of polyubiquitination of E1A by TRIM35 (Fig. 4G). E1A and TRIM35-V5 have cotransfected with WT HA-Ub or its mutants

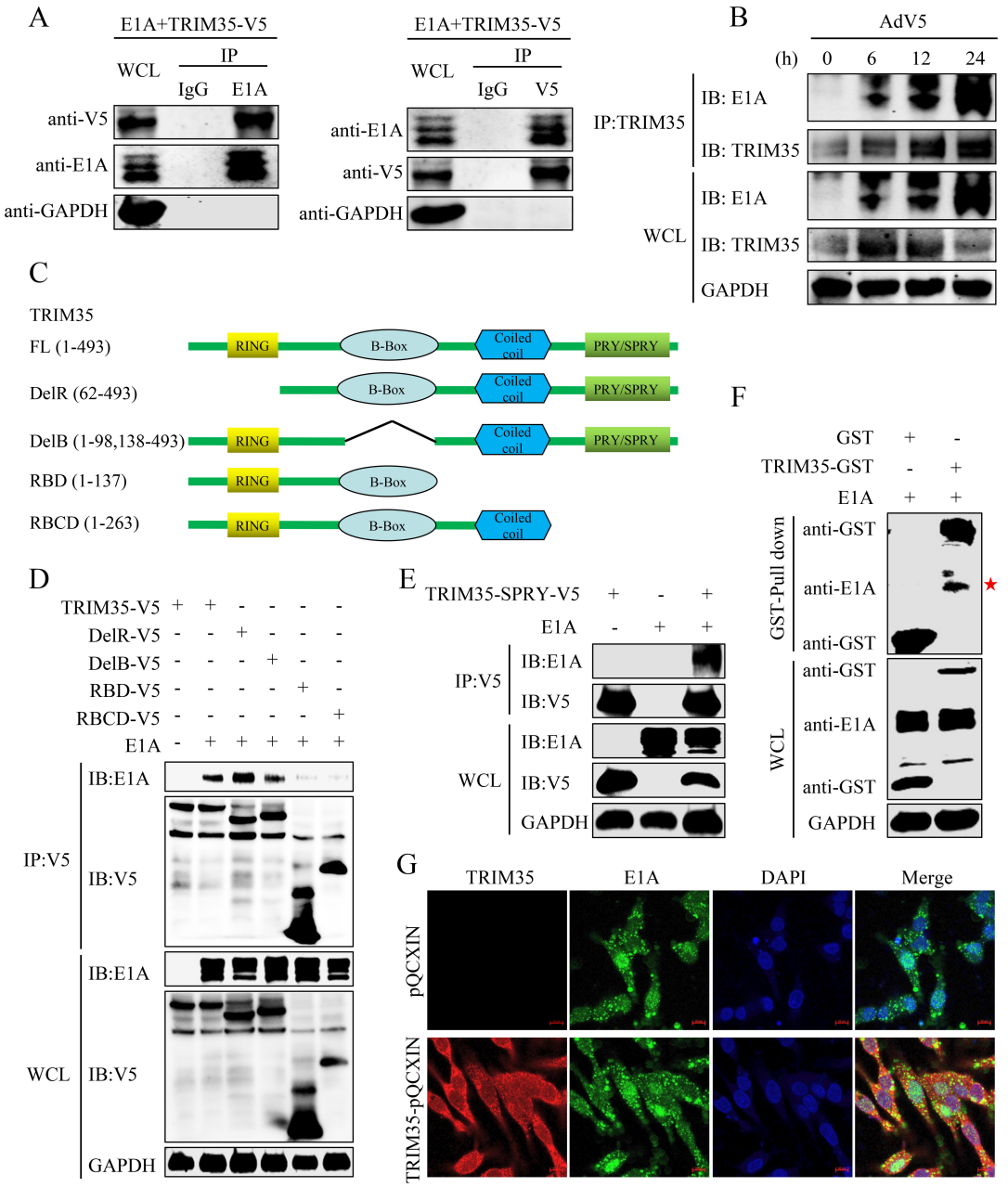

FIG 3 TRIM35 interacts and colocalizes with E1A. (A) TRIM35-V5 was cotransfected with E1A from the HAdV-C5 into HEK293T cells. The cell lysates were immunoprecipitated (IP) using an anti-E1A antibody (left panel), anti-V5 antibody (right panel), or control IgG and blotted as indicated. (B) HAdV-C5 infected A549 cells with an MOI of 20 during normal infection. Cell lysates were collected at specified time points and immunoprecipitated using an anti-TRIM35 antibody. (C) Truncated expression mutant diagram of TRIM35. (D) E1A and V5-tagged TRIM35 mutants were cotransfected into HEK293T cells. The cell lysates were immunoprecipitated using an anti-V5 antibody and detected with a western blot. (E) V5-tagged TRIM35 PRY/SPRY domain and E1A were transiently cotransfected into HEK293T cells and determined using co-IP and western blot. (F) The interaction between E1A and TRIM35 was detected with the GST pull-down assay. HEK293T cells were transiently transfected with GST or GST-TRIM35. After 36 h of transfection, the cell lysate was collected and incubated with Glutathione Sepharose 4 Fast Flow for 6 h. The cell lysates expressing pcDNA3.1-E1A were mixed. Subsequently, unbound proteins were washed away and western blots were conducted. (G) HAdV-C5 infected control A549 cells or TRIM35-overexpression A549 cells with an MOI of 20 for 8 h to identify their colocalization. The cells were fixed using 4% paraformaldehyde, incubated with anti-E1A and anti-TRIM35 antibodies, and finally analyzed by confocal microscopy. At least three independent experiments were conducted.

into HEK293T cells. The results showed that TRIM35-mediated E1A polyubiquitination could be identified in the presence of HA-K48-Ub, but other HA-Ub mutants could not (Fig. 4H). Coimmunoprecipitation analysis revealed that TRIM35 promoted E1A

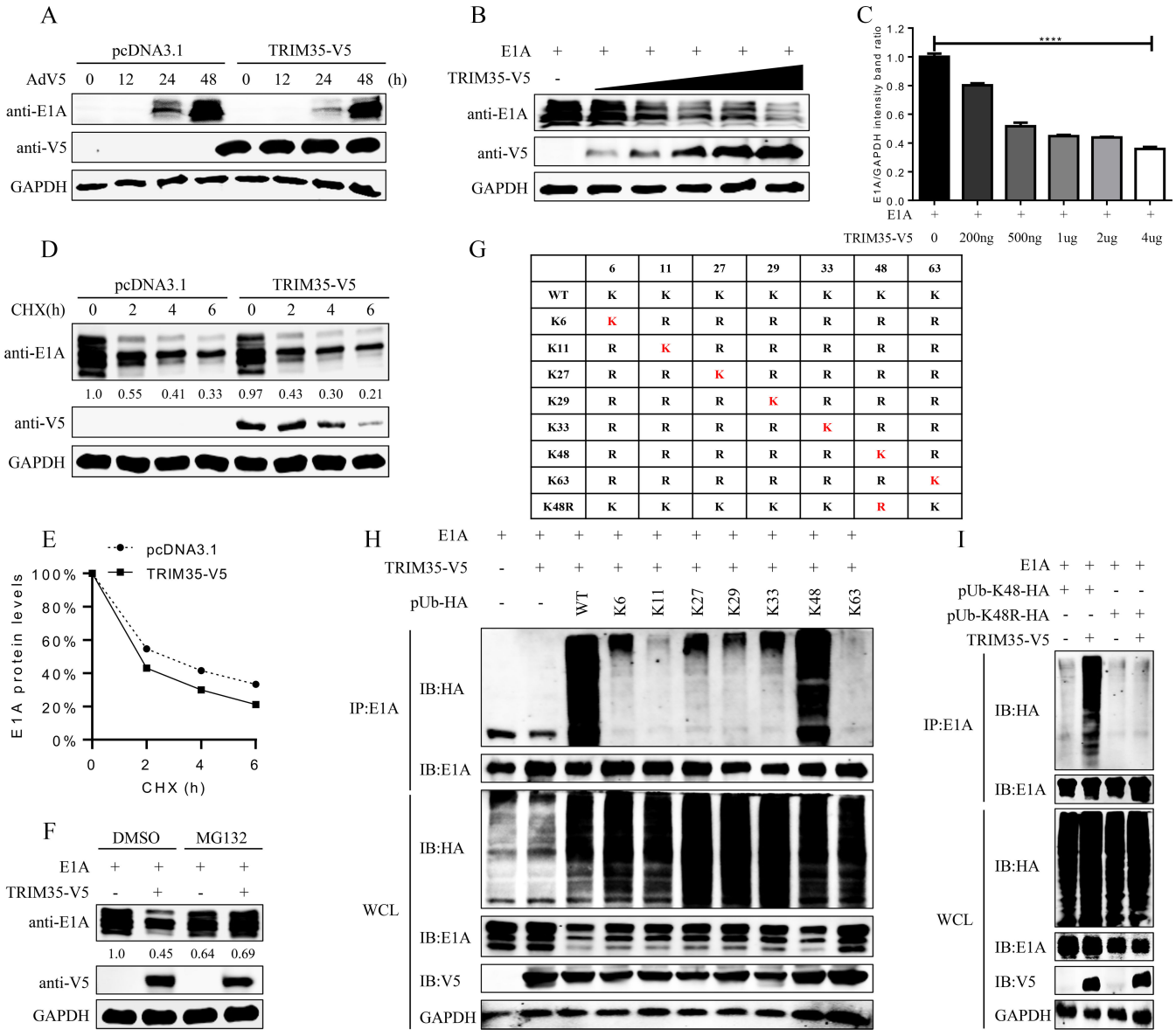

FIG 4 TRIM35 ubiquitinates and degrades E1A. (A) IB analysis of HEK293T cells expressing TRIM35-V5 or control vector for 24 h, followed by HAdV-C5 infection. (B) HEK293T cells were cotransfected with E1A and gradually increased TRIM35-V5. The cell lysates were immunoblotted with specified antibodies. (C) Gray value calculation of three independent experiments in (B). ****, $P < 0.0001$. (D) TRIM35-V5 or pcDNA3.1 were cotransfected with E1A for 48 h and then treated with 20 µg/mL cycloheximide for 0, 2, 4, or 6 h. Whole-cell lysates were blotted using indicated antibodies. (E) Quantification of relative E1A levels is shown in the bottom panel. (F) E1A was cotransfected with vector or TRIM35-V5 into HEK293T cells. After 24 h, cells were treated with dimethyl sulfoxide or 10 µM MG132 for 12 h. The cell lysates were blotted with the indicated antibodies. (G) Depiction of ubiquitin molecules and their mutation sites. (H) E1A, TRIM35-V5, and pHA-Ub WT or mutants (K6, K11, K27, K29, K33, K48, or K63) were cotransfected into HEK293T cells. Ubiquitination and immunoblotting experiments were performed using indicated antibodies. (I) HEK293T cells were cotransfected with E1A, TRIM35-V5, and pHA-Ub mutants (K48, K48R). Then, ubiquitination assays were performed and blotted with indicated antibodies. At least three independent experiments were conducted.

ubiquitination only in the presence of the K48 ubiquitin mutant but not in the presence of the K48R ubiquitin mutant (Fig. 4I). Thus, TRIM35 catalyzes K48-linked E1A polyubiquitination.

Ubiquitin E3 ligase activity is needed for TRIM35 antiviral function

Based on previous studies, TRIM35 can degrade E1A protein through K48 ubiquitination. Thus, we explored which domain of TRIM35 is involved in degradation. The RING

domain is critical for the E3 ligase activity of TRIM proteins (29, 30). E1A was transfected with the TRIM35 RING deletion (DelR) mutant into HEK293T cells to define the role of ligase activity of TRIM35 in the E1A protein. The DelR mutant did not decrease E1A protein expression (Fig. 5A), suggesting that the RING domain in TRIM35 mediated E1A ubiquitination and degradation. Therefore, the role of the RING domain in TRIM35-mediated viral restriction was evaluated. First, we transduced retrovirus encoding TRIM35 RING deletion (DelR) mutant into A549 cells to develop the RING deletion (DelR) overexpression stable cell lines and then infected with HAdV-C5. TCID50 assay revealed that the mutant could not inhibit HAdV-C5 replication compared to the control A549 cells. In contrast, the TRIM35-overexpressing A549 cells could inhibit HAdV-C5 replication (Fig. 5B). In another experiment, the HAdV-C5-GFP virus (HAdV-C5-GFP) infected the control, DelR-overexpressing, and TRIM35-overexpressing A549 cells. The assay revealed that the RING deletion (DelR) mutant is not resistant to HAdV-C5 infection (Fig. 5C). Moreover, *in vitro* ubiquitination assay indicated that TRIM35 elevated the E1A ubiquitination levels in the presence of HA-K48-Ub. However, ectopic expression of the RING deletion mutant showed little or no effect on E1A ubiquitination (Fig. 5D). Therefore, the antiviral function of TRIM35 needs E3 ubiquitin ligase activity (31).

The E3 ligase activity of TRIM proteins requires cysteine (C) residues in their RING domain (32, 33). The RING domain of TRIM35 has eight cysteine residues (23). We performed *in vitro* ubiquitination experiments to determine which cysteine residues are essential for E1A polyubiquitination in the RING domain of TRIM35. The results indicated that the polyubiquitination of E1A by TRIM35 mutant C21S was significantly decreased compared with WT TRIM35 (Fig. 5E). Thus, the C21S mutation in the TRIM35 RING domain is essential in the antiviral response.

E1A K253 and K285 are the crucial sites for TRIM35-mediated degradation

The ubiquitin binding to receptor lysine residues on substrate proteins is essential in ubiquitination (26, 34). Three lysine residues have been identified among the HAdV-C5 E1A protein (35) (Fig. 6A). We constructed E1A mutants containing single, double, or three arginine mutations to identify the specific E1A lysine residue for TRIM35 ubiquitination. HEK293T cells were cotransfected with V5-tagged TRIM35 and Flag-tagged E1A or its mutants. Western blot results indicated that when the K253R and K285R sites of E1A mutated simultaneously, e.g., K253/285R and K208/253/285R, the E1A protein expression level was significantly complemented than in WT E1A, while other E1A mutants did not (Fig. 6B and C). Moreover, K253/285R residues were the major degradation sites on HAdV-C5 E1A. As expected, gradually increased TRIM35 does not affect the expression of E1A K253/285R mutants (Fig. 6D). Furthermore, ectopic expression of TRIM35 had little or no effect on the ubiquitination of E1A K253/285R mutants (Fig. 6E). Besides, this modification occurred in the cytosol, possibly blocking E1A nuclear import in addition to causing degradation (36). Next, we detected the effect of TRIM35 on the WT E1A and the E1A mutant (K208, K253, and K285R) acetylation levels. The data indicated that TRIM35 has no effect on the acetylation of E1A (Fig. 6F). We also examined whether TRIM35 affects the interaction between E1A and importin α3 (36). The results depict that TRIM35 does not affect E1A and importin α3 binding, with no blocking nuclear import of E1A (Fig. 6G). Our data indicate that TRIM35 mediates E1A polyubiquitination and degradation at the K253/285R site, providing a versatile way to combat HAdV-C5 infection.

Schematic diagram of the oncolytic adenovirus expressing a short-hairpin RNA against TRIM35 (shTRIM35) genome

Serotype 2 and 5 species C viruses have been investigated at viral gene function, gene regulation, replication, and host–virus interaction levels (37, 38). Due to the depth of reagents from early Ad studies, gene therapy, vaccine development, and oncolytic Ad vector development were initially based on the Ad5 serotype (39–42). To further validate whether our hypothesis and findings are relevant for cancer therapy with oncolytic

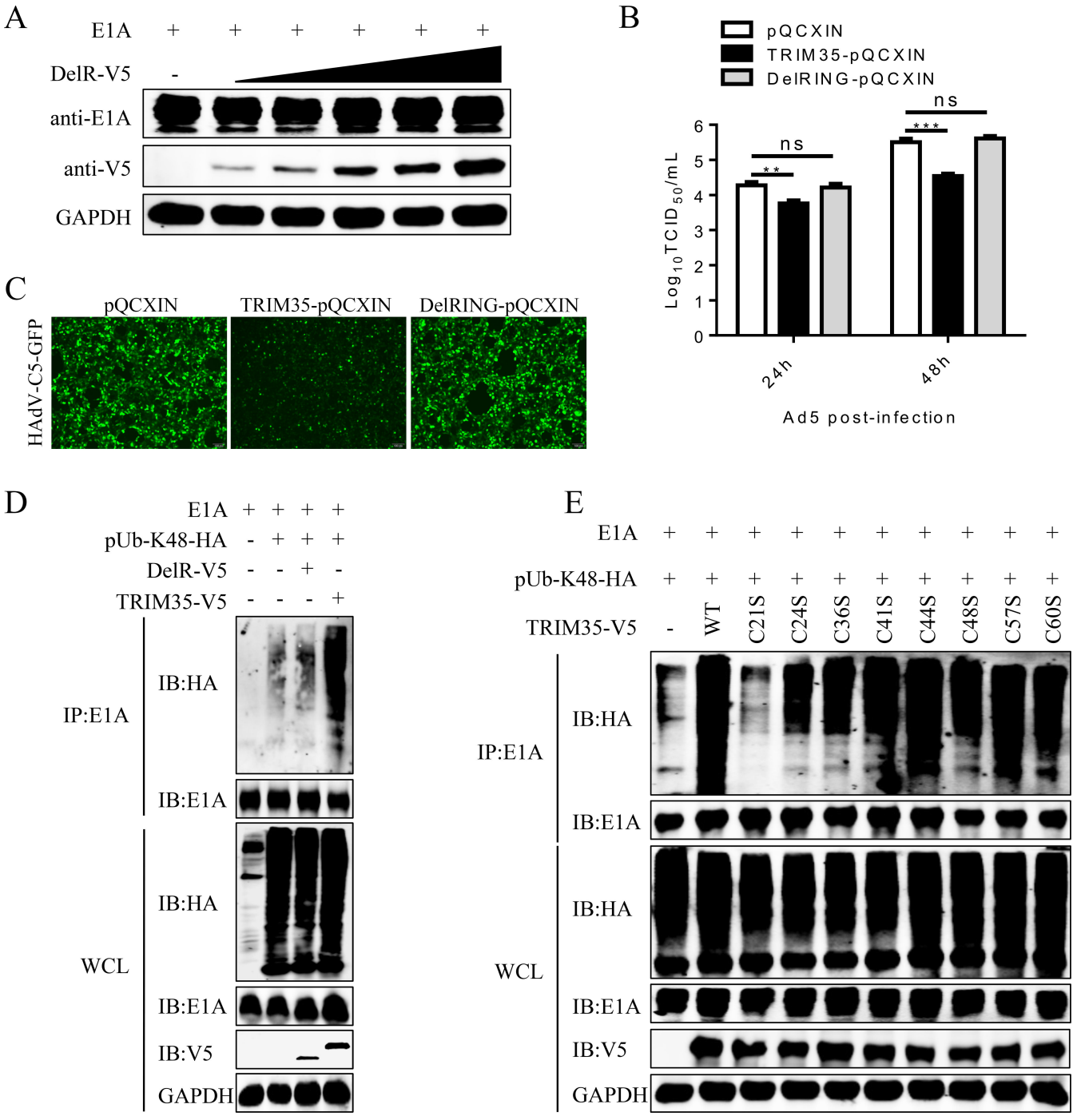

FIG 5 TRIM35 needs E3 ligase activity for antiviral function. (A) E1A and gradually increased RING deletion (DelR) mutants were cotransfected into HEK293T cells. Then, cell lysates were blotted using indicated antibodies. (B) DelR-overexpressing, TRIM35-overexpressing, or control A549 cells were infected with HAdV-C5 at an MOI of 5. The supernatant was collected at specified time points, and the virus titer was determined using TCID50 assay on HEK293 cells. All experiments were repeated at least three times. (C) Observation of virus-infected cells using a fluorescence microscope, as described in (B) with the HAdV-C5-GFP virus. Scale bars, 100 µm. (D) HEK293T cells were cotransfected with E1A and empty vector, TRIM35-V5 or DelR mutant with V5 tag, then treated with 10 µM MG132 for 12 h to prevent E1A protein degradation. The cell lysates were collected for immunoprecipitation using an anti-E1A antibody, and immunoblotting was performed using specified antibodies. (E) E1A, HA-K48-Ub, and V5-tagged TRIM35 or its mutants were cotransfected into HEK293T cells and immunoprecipitated using an anti-E1A antibody. The ubiquitination of E1A was detected via immunoblotting with indicated antibodies. At least three independent experiments were conducted.

adenoviruses, a recombinant oncolytic adenovirus carrying shTRIM35 was constructed (Fig. 7A). A more severe cytopathic effect caused by OAV-shTRIM35 infection could be

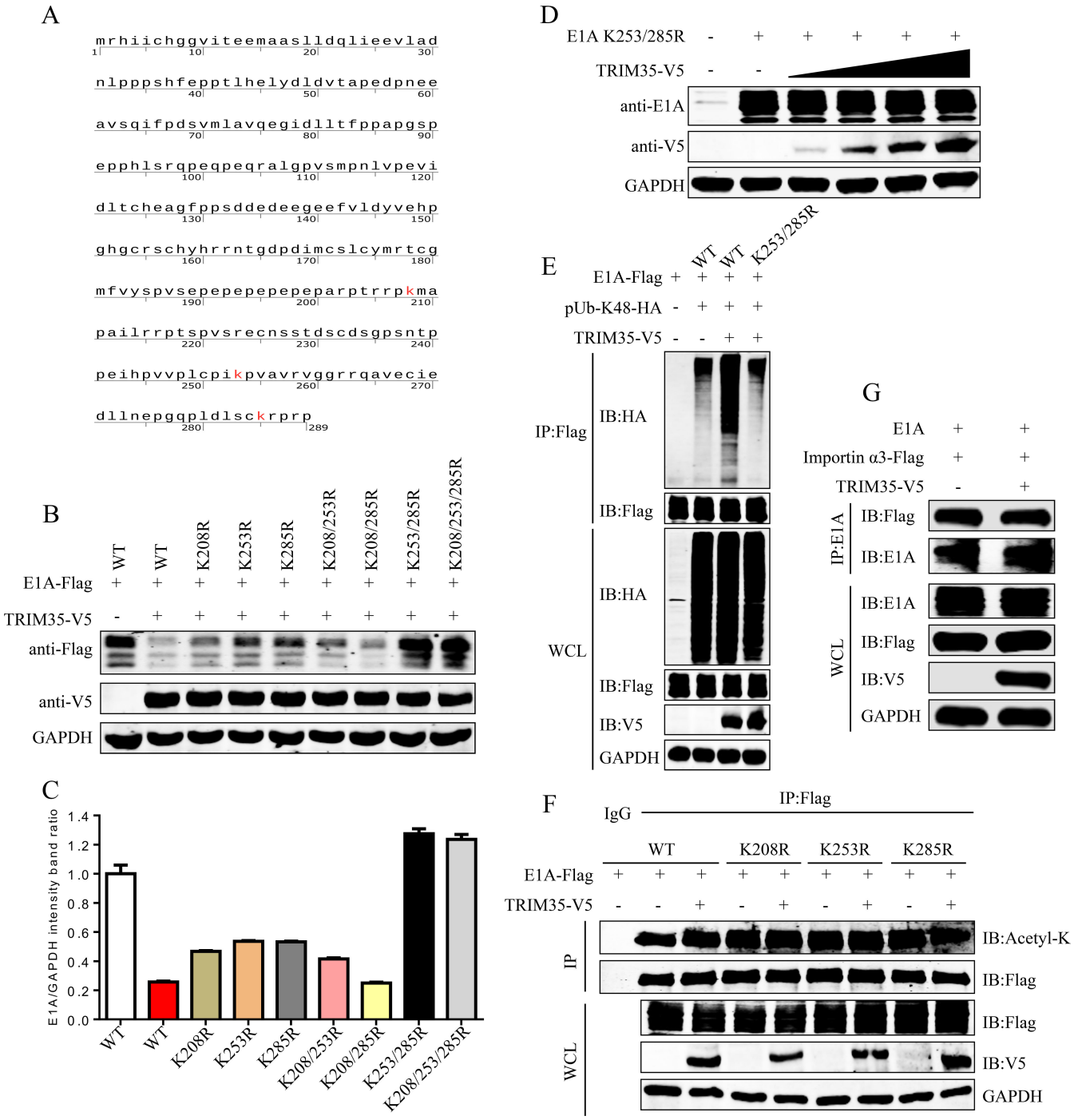

FIG 6 E1A K253 and K285 are the crucial sites for TRIM35-mediated degradation. (A) Amino acid mapping of adenovirus type 5 E1A protein, red-labeling lysine K. (B) Different lysine mutants of HAdV-C5 E1A protein were constructed and analyzed by western blot. (C) Gray value calculation of the three independent experiments in (B). (D) HEK293T cells were cotransfected with E1A K253/285R and gradually increased TRIM35 for 36 h. Cell lysates were blotted with specified antibodies. (E) TRIM35-V5, HA-K48-Ub, and Flag-tagged HAdV-C5 E1A WT or K253/285R mutant were cotransfected into HEK293T cells, and the cells were collected for immunoprecipitation to detect K48-linked ubiquitination of E1A. (F) HEK293T cells were cotransfected with WT E1A and mutants (K208R, K253R, and K285R), together with TRIM35-V5, for 36 h. The indicated antibodies were used to detect the immunoblot results of acetylated E1A. (G) HEK293T cells were transfected with plasmids expressing E1A, Flag-tagged importin α3, and TRIM35-V5. The cell lysates were immunoprecipitated using a mouse anti-E1A mAb, and the bound proteins were detected via western blotting with the specified antibodies. At least three independent experiments were conducted.

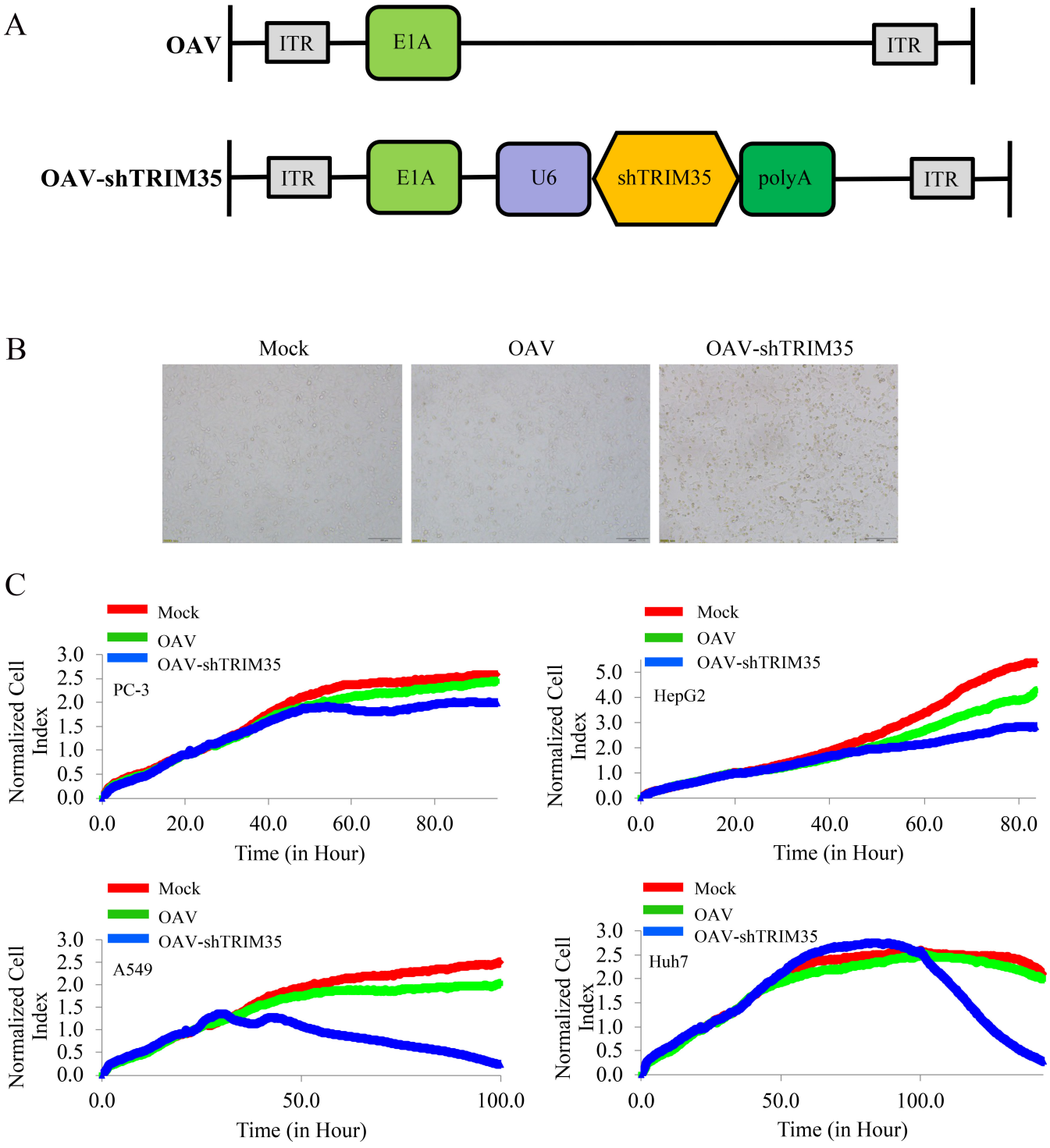

FIG 7 Schematic diagram of the oncolytic adenovirus expressing a short-hairpin RNA against TRIM35 (shTRIM35) genome. (A) The construction diagram of OAV-shTRIM35. (B) A549 cells were infected with OAV-shTRIM35 or OAV at an MOI of 10. The tumor-killing effect was observed at 36 h post-infection using the microscope. (C) The anti-proliferative effects of OAV and OAV-shTRIM35 on PC-3, A549, HepG2, and Huh7 cells were analyzed using RTCA. At least three independent experiments were conducted.

observed in A549 cells than in OAV) with an MOI of 10 at 36 h post-infection (Fig. 7B). The data indicated that OAV-shTRIM35 showed a more substantial oncolytic effect *in vitro*. In addition, real time cell analysis (RTCA) revealed that OAV-shTRIM35 had a better anti-proliferative effect on different tumor cells (Fig. 7C). OAV-shTRIM35 has a more significant

oncolytic activity than traditional OAVs, facilitating subsequent modification and application of oncolytic adenovirus.

Effect of ectopic shTRIM35 expression on oncolytic activity *in vivo*

PC-3 cells were used to establish tumor models and characterize the oncolytic effects of OAV-shTRIM35. When the subcutaneous tumor diameter was about 5 mm, mice were randomly divided into three groups: PBS, OAV, and OAV-shTRIM35 ($n = 5$). The virus was intratumorally injected every other day with three injections, with a total dose of 1×10^9 PFU. The scheme of the treatment schedule is depicted in Fig. 8A. The intratumoral administration of OAV-shTRIM35 demonstrated antitumor activity compared with the saline or OAV-treated group, with tumor growth inhibition of 78.56% for the PC-3 cell cancer model (Fig. 8B, C, and D). Additionally, OAV-shTRIM35 significantly reduced the tumor volume (Fig. 8E). Three mice were sacrificed from each group on Day 7 after administration, and genomic DNA was extracted from tumor tissues. Real-time PCR was used to detect the content of the viral genome. The data indicated that tumors treated with OAV-shTRIM35 had more high-level viral expression than OAV (Fig. 8F). More E1A protein was also detected in OAV-shTRIM35 (Fig. 8G). The data indicated that OAV-shTRIM35 could induce a sufficient antitumor effect against prostate carcinoma *in vivo*.

DISCUSSION

HAdVs represent a ubiquitous and clinically significant pathogen without an effective antiviral treatment (43). Human adenovirus can cause severe diseases that can be fatal in some populations. No FDA-approved drugs are available to treat adenovirus infections (44, 45), and current antiviral research is very definite. The "one drug, one bug" method of direct antiviral has significant limitations since most currently approved antiviral drugs are enzymes targeting the virus. Moreover, the activity range of these enzymes is very narrow and insufficient to resist virus diversity (44–46). So, developing antiviral drugs with a wide range of effects is very meaningful. Targeting virus-dependent host factors is one way to establish broad-spectrum antiviral drugs (47).

Many proteins have significant roles in different stages of the viral life cycle to regulate antiviral responses. TRIM family members are the most studied innate or intrinsic antiviral factors (13, 15, 17). The direct interaction between the host factors and viruses is disrupted by innate immunity to weaken viral infection (47). Some TRIM proteins, such as TRIM22, TRIM32, and TRIM25, have been reported as intrinsic limiting factors (18, 21, 48). Similarly, our study revealed that TRIM35 ubiquitinates and directly degrades E1A to inhibit adenovirus infection. Therefore, TRIM35 is a new intrinsic immune factor inhibiting HAdV infection.

Ubiquitin (Ub) is widely distributed in eukaryotes and is a highly conserved protein with 76 amino acids. The seven lysine residues K6, K11, K27, K29, K33, K48, and K63 are vital in the Ub function, each acting as an Ub target to connect to another Ub (12). K48-linked polyubiquitination is the most well-understood ubiquitination targeting protein degradation via the 26S proteasome (49, 50). Other ubiquitination-like modifications have been gradually discovered, including sumoylation, ISGylation, neddylation, palmitoylation, and acetylation (51–54).

As ubiquitin E3 ligases, TRIM35 consists of RING, B-box, a coiled-coil domain, and a multifunctional C-terminal domain (22, 23). The C-terminus of TRIM35 consists of a SPRY domain and belongs to a subgroup of the TRIM family. We demonstrated how TRIM35 affects HAdV infection. TRIM35 overexpression significantly negatively affects viral growth and decreases early viral gene expression. Further studies revealed that E1A interacts with the SPRY domain of TRIM35. Then the E1A and TRIM35 interaction was confirmed to be direct via GST pull-down assay.

E1A is essential in the life cycle of HAdV (55, 56). Once the virus is infected, the cell protein will catalyze the E1A transcription process (57). E1A protein can stimulate the transcription of other early HAdV-C5 mRNAs, which is necessary to synthesize other viral

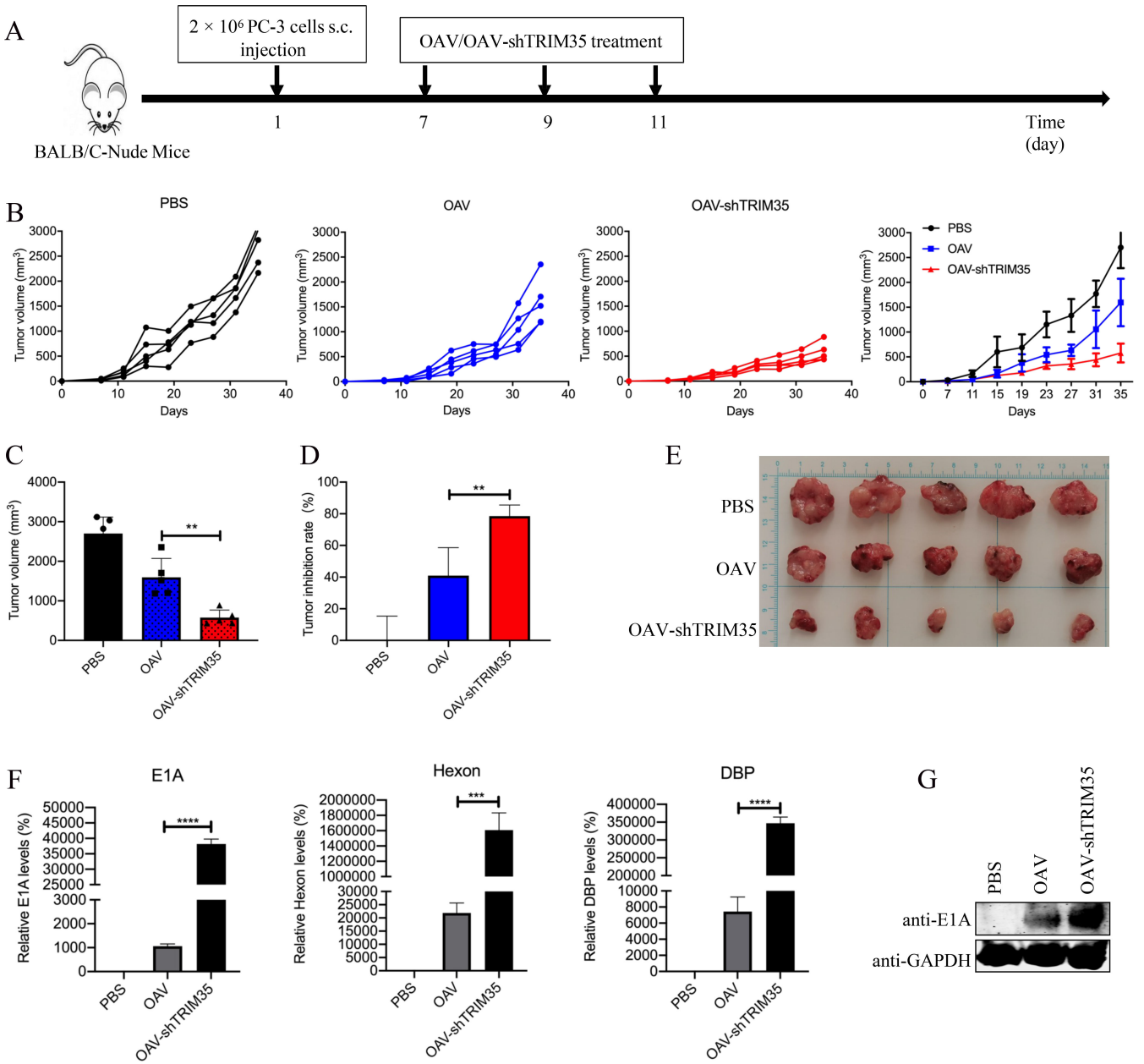

FIG 8 Effect of ectopic shTRIM35 expression on oncolytic activity *in vivo*. (A) Experimental timeline for *in vivo* studies as shown. Nude mice were subcutaneously inoculated with PC-3 cells of 2×10^6 cells per mouse ($n = 5$ per group). When tumors reached about 50 mm^3, tumors were directly injected with PBS, OAV, or OAV-shTRIM35 (1×10^9 PFU) every other day for three injections. (B) The tumor growth curves of each mouse were displayed. (C) The mean tumor volume curves ± SD were displayed. (D) Tumor inhibition rates in different groups are represented. (E) The size of the tumor mass in each different group is shown. (F and G) E1A, Hexon, and DBP viral gene expression in tumor tissues were detected on day 7 after three times of OAV/OAV-shTRIM35 treatments. Then, the E1A viral protein expression was detected in the tumor through a western blot. **, $P < 0.01$; ***, $P < 0.001$; ****, $P < 0.0001$.

proteins (58, 59). The early viral E2A gene encodes a single-stranded DNA binding protein, HAdV DBP, essential for viral genome replication (56). The time-course analysis of transcription indicated that TRIM35 interfered with the expression of HAdV-C5 early genes E1A and DBP during infection. We also observed that the antiviral activity of TRIM35 required E3 ligase activities. These results align with previous findings that TRIM35 could inhibit the production of the infectious progeny of the influenza virus (23). Furthermore, TRIM35 mediates the degradation of E1A through K48-linked ubiquitination, suppressing HAdV replication (Fig. 9).

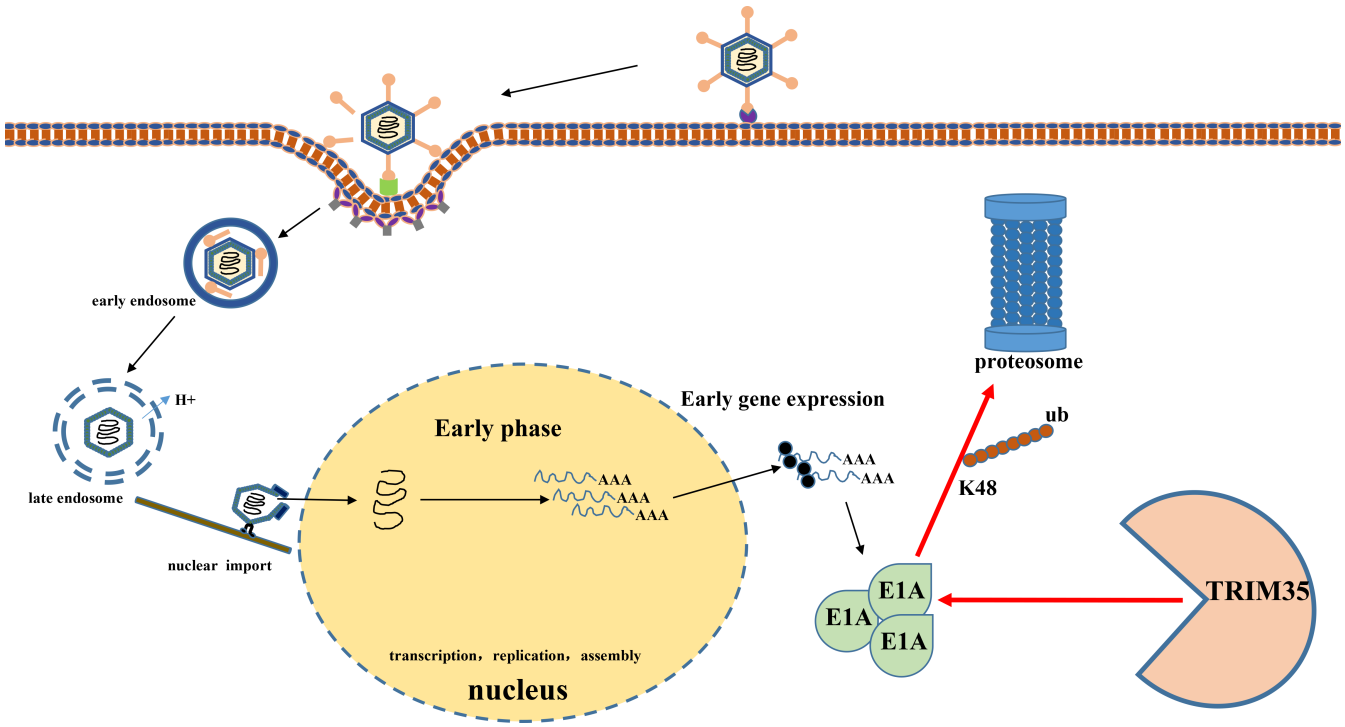

FIG 9 Schematic model of TRIM35-mediated inhibition in HAdV-C5 infection by degrading E1A. E1A is transported from the nuclear pore into the nucleus in the cytoplasm. In the presence of TRIM35, E1A could be degraded via Lys48-linked polyubiquitination, delaying the virus life cycle.

Recombinant adenoviruses have been extensively investigated and used in clinical trials for cancer and vaccines, such as replication-defective adenovirus vectors and conditional replication adenoviruses (60–62). Replication-defective adenovirus vector has been used in cancer gene therapy *in vivo* (41, 63, 64). Extensive primary research and clinical trials have proved safe but ineffective (65, 66). Combined with our findings that TRIM35 could effectively mediate the replication and transcription of adenovirus, a novel oncolytic adenovirus expressing shRNA targeting TRIM35 was constructed, confirming its better oncolytic effect *in vivo*. Our findings provide new strategies and significant implications to enhance the efficiency of Ad-based therapy.

In summary, we demonstrated for the first time that E1A interacts with E3 ligase TRIM35 during HAdV infection. Moreover, TRIM35 inhibits HAdV replication and targets E1A for proteasome degradation, indicating that TRIM35 is a potent antiviral during HAdV infection. Managing this natural defense pathway could provide a potential strategy for regulating HAdV infection.

MATERIALS AND METHODS

Cells and viruses

HEK293 cells, HEK293T cells, Huh7 cells, and HepG2 cells were maintained in Dulbecco's modified Eagle medium with antibiotics and 10% fetal bovine serum. A549 cells were cultured in F-12K medium plus 10% fetal bovine serum. PC-3 cells were cultured in 1,640 medium plus 10% fetal bovine serum. All the cells were tested for mycoplasma contamination.

The HAdV-C5 virus expressing wt E1A was preserved in our laboratory. A549 cells were infected with different MOI of plaque-forming units (PFU)/mL. Cells were cultured to about 70% confluence and infected for 2 h at 37°C. Samples were collected at

specified time points for downstream experiments. The virus titer was determined using the 50% tissue-culture infectivity endpoint (TCID50) method of Reed and Muench (67).

Adenovirus construction

The U6-promoter-driven TRIM35 shRNA was synthesized by Azenta Life Sciences and cloned into the adenoviral shuttle plasmid pZD55. pZD55-TRIM35 shRNA was cotransfected into HEK293 cells with adenoviral cytoskeleton plasmid pBHGE3 using Lipofectamine 2000 according to the manufacturer's instructions (63). The packaged adenovirus Ad5-ZD55-TRIM35 shRNA was amplified in HEK293 cells. Then, the virus was collected, and the titer was measured with the 50% tissue-culture infectivity endpoint (TCID50) method.

Plasmids and antibodies

Vectors with cytomegalovirus (CMV) promoters are used to construct all plasmids. Full-length E1A was built into pcDNA3.1. Plasmids expressing the V5-tagged TRIM35 gene were described previously (23). The TRIM35 mutant constructs were generated through PCR mutagenesis. All the plasmid constructs were confirmed using DNA sequencing.

Antibodies included were: anti-GAPDH (10494–1-AP; Proteintech), anti-E1A (05–599; Millipore), anti-TRIM35 (SAB2103161A; Sigma Aldrich), anti-HA (51064–2-AP; Proteintech), anti-V5 (V8012, V8137; Sigma Aldrich), anti-GST (10000–0-AP; Proteintech), anti-Flag (F1804, F7425; Sigma Aldrich), Pan Acetylation Monoclonal antibody (66289–1-Ig; Proteintech), and Mouse IgG (A7028; Beyotime). Alexa Fluor 633 goat anti-mouse IgG (H + L) (A21050) and Alexa Fluor 488 donkey anti-rabbit IgG (H + L) (A21206) were procured from Life Technologies. DyLight 800 goat anti-mouse IgG (H + L) (072–07-18-06) and DyLight 800 goat anti-rabbit IgG (H + L) (072–07-15-06) were provided by KPL. The antibody was diluted according to the standard protocol for western blot and immunofluorescence.

Coimmunoprecipitation and western blotting

NP-40 lysis buffer (150 mM NaCl, 50 mM Tris-HCl pH 7.5, 0.1% NP-40) was used to lyse cells with a protease inhibitor cocktail. Centrifugation was performed at 4°C 12,000 × *g* for 15 min, and the lysates were collected. The supernatants were denatured in 5× sample loading buffer for 10 min at 95°C. The supernatant and the corresponding primary antibody for immunoprecipitation assays were incubated overnight at 4°C in the presence of protein G-agarose (Roche), followed by western blotting.

GST pull-down assay

GST pull-down was performed as described previously (23, 24). First, GST or GST-TRIM35 fusion protein was purified and mixed with lysates from cells expressing E1A overnight at 4°C. The GST-agarose dragged protein was detected using the western blot with mouse anti-E1A and rabbit anti-GST antibodies.

Ubiquitination assay

HEK293T cells were cotransfected with E1A and pHA-Ub, with or without TRIM35-V5. The cells were treated with 10 µM MG132 (Sigma-Aldrich) for 12 h. Then, the cells were lysed using NP-40 lysis buffer with a deubiquitinase inhibitor (10 µM *N*-ethylmaleimide; Sigma-Aldrich). Next, anti-E1A antibodies were added to the samples separately. Subsequently, the samples were incubated overnight at 4°C and were detected using the western blot with the specified antibody.

Immunofluorescence assay

The cells were fixed with 4% paraformaldehyde for 30 min at room temperature, permeabilized using 0.5% Triton X-100, and blocked with 3% BSA phosphate-buffered saline (PBS). The primary antibodies (rabbit α-TRIM35, mouse α-E1A) were incubated for 1 h at room temperature, and the secondary antibodies (Alexa Fluor 488, Alexa Fluor 633; Life Technologies) were incubated for 40 min at room temperature. Confocal images were obtained using a Zeiss LSM880 scanning confocal microscope (Zeiss Microsystems).

Real-time gene expression analysis

Total RNA was extracted at the indicated time points under the manufacturer's instructions with the TRIzol reagent (Invitrogen). Total RNA was used to perform reverse transcription reactions according to the manufacturer's guidelines. Subsequently, the cDNA was used for real-time expression analysis using the SYBR Green PCR Master Mix (Takara) with a LightCycler 480 II system (Roche). Relative RNA quantities were determined with the ΔΔCt method and normalized to GAPDH mRNA levels. Table S1 lists the specific primers for real-time PCR. Student's *t*-test was used for statistical analysis and significance determination of real-time expressions.

siRNA knockdown

siRNA knockdown was conducted as described previously (24). The TRIM35-specific silencer siRNA was transfected into A549 cells with RNAiMax reagent (Life Technologies) based on the manufacturer's specifications, with a final concentration of 10 nM siRNA. Silencer Select negative-control siRNA was used as the negative siRNA control. Table S2 lists the siRNA sequences for transient silencing of human TRIM35 or scrambled siRNA obtained from Gene Pharma.

Cell viability

Cell viability was determined with the Cell Counting Kit–8 (Sigma). The cells were seeded into a 96-well plate. Cell viability was measured according to the manufacturer's instructions.

Virus replication assay

All viruses were amplified in HEK293 cells with low passages, and virus titers were determined in HEK293 cells. All the infections were performed in a serum-free medium. A549 lung epithelial cancer cells were infected with HAdV-C5 at a specific multiplicity of infection. They were collected at different time points post-infection to determine the virus titer. All the experiments were conducted in a biosafety level 2 laboratory.

In vivo tumor study

All the animal experiments were performed under protocols approved by the Institutional Animal Care and Use Committee of Xuzhou Medical University. For human tumor xenograft studies, PC-3 cells (2×10^6 cells per mouse) were prepared and injected subcutaneously within the right flank of male Balb/c nude mice (purchased from GemPharmatech Co. Ltd., Nanjing, China). We used caliper measurement to monitor tumor growth and body weight of mice twice or three times per week. Tumor volume was determined using the formula length × width^2 × 0.5. Once tumor volumes reached 50–100 mm^3, PBS, oncolytic adenovirus OAV or OAV-shTRIM35 was intratumorally administered for three injections every other day at 1×10^9 PFU per mouse. After 7 days of treatment, tumors were collected from three mice for each group and analyzed using qRT-PCR and western blotting to determine the expression of adenoviral E1A, Hexon, and DBP.

Mass spectrometry

Whole-cell lysate protein (250 µg for each sample) was digested according to the FASP procedure. Briefly, the detergent, DTT, and other low-molecular-weight components were removed using 100 µL UA buffer by repeated ultrafiltration facilitated by centrifugation. The protein suspension was digested with 5 µg trypsin in 100 µL 25 mM NH_4HCO_3 overnight at 37°C. After digestion, the peptides in each sample were desalted on C18 cartridges, concentrated by vacuum centrifugation, and reconstituted in 40 µL of 0.1% (vol/vol) formic acid. Liquid chromatography-tandem MS (LC-MS/MS) analysis was performed on a Q-Exactive mass spectrometer (Thermo Fisher Scientific) that was coupled to Easy nLC (Proxeon Biosystems, now Thermo Fisher Scientific) for 120 min with the help provided by Shanghai Applied Protein Technology (Shanghai, China).

The MS data were analyzed using MaxQuant software (version 1.6.14) and were searched against the UniProt proteome database. The label-free quantitation algorithm was performed for quantitative analysis. Quantifiable proteins were defined as those identified at least twice in the three biological replicates. Proteins with an adjusted *P* value <0.05 and abundance fold change >2 were assigned as differentially expressed between the empty vector and adenovirus E1A overexpression (Table S3).

Statistical analysis

All experiments were performed at least three times. The sample size was sufficient for data analysis using paired two-tailed Student's *t*-tests. All the statistical analyses had significance at $P < 0.05$.

ACKNOWLEDGMENTS

Conceptualization, Nan Sun and Jikai Zhang; methodology, Nan Sun and Jikai Zhang; data curation, Nan Sun, Lin Fang and Jikai Zhang; writing—original draft preparation, Nan Sun and Jikai Zhang; writing—review and editing, Nan Sun, Lin Fang, Gang Wang, and Jikai Zhang. All authors have read and agreed to the published version of the manuscript.

This work was supported by the National Key R&D Program of China (2018YFA0900900), National Natural Science Foundation of China (32200124), Natural Science Foundation of Jiangsu Province of China (BK20210901), Natural Science Research of Jiangsu Higher Education Institutions of China (21KJB310008, 21KJB320020), and Xuzhou Medical University (D2020031, D2020046).

AUTHOR AFFILIATIONS

[1]Xuzhou Medical University, Xuzhou, China
[2]Jiangsu Center for the Collaboration and Innovation of Cancer Biotherapy, Cancer Institute, Xuzhou Medical University, Xuzhou, China
[3]Center of Clinical Oncology, Affiliated Hospital of Xuzhou Medical University, Xuzhou, China

AUTHOR ORCIDs

Gang Wang http://orcid.org/0000-0001-6020-7263

FUNDING

Funder	Grant(s)	Author(s)
MOST | National Key Research and Development Program of China (NKPs)	2018YFA0900900	Jun nian Zheng
MOST | National Natural Science Foundation of China (NSFC)	32200124	Nan Sun

Funder	Grant(s)	Author(s)
Natural Science Foundation of Jiangsu Province (Jiangsu Natural Science Foundation)	BK20210901	Jikai Zhang
JPDE | Natural Science Research of Jiangsu Higher Education Institutions of China (Natural Science Foundation of Colleges and Universities in Jiangsu Province)	21KJB320020	Nan Sun Jikai Zhang
Xuzhou Medical University (XZMU)	D2020046	Nan Sun Jikai Zhang

AUTHOR CONTRIBUTIONS

Nan Sun, Conceptualization, Data curation, Funding acquisition, Investigation, Project administration, Supervision, Writing – original draft, Writing – review and editing | Jikai Zhang, Conceptualization, Data curation, Funding acquisition, Investigation, Writing – original draft | Chen Zhang, Formal analysis, Investigation | Tan Xie, Investigation | Zeyu Zhang, Investigation | Xueyan Wang, Investigation | Wanjing Li, Investigation | Yi Zhang, Investigation, Methodology | Zhaokai Chen, Investigation | Junnian Zheng, Conceptualization, Funding acquisition, Project administration, Writing – review and editing | Lin Fang, Project administration, Software, Writing – review and editing | Gang Wang, Conceptualization, Project administration, Supervision, Writing – review and editing

ADDITIONAL FILES

The following material is available online.

Supplemental Material

Fig. S1 and S2 (JVI00700-23-S0001.docx). The expression of endogenous E1A in HEK293T cells was detected in Fig S1. The expression of TRIM35 during adenovirus infection was examined in Fig S2.
Table S3 (JVI00700-23-S0002.docx). Analysis of differential results of E1A proteomics.
Tables S1 and S2 (JVI00700-23-S0003.xlsx). Table S1: Primers used for RNA quantification. Table S2: SiRNAs are used for gene silencing.

REFERENCES

1. Lion T. 2014. Adenovirus infections in immunocompetent and immunocompromised patients. Clin Microbiol Rev 27:441–462. https://doi.org/10.1128/CMR.00116-13
2. Shieh WJ. 2022. Human adenovirus infections in pediatric population - an update on clinico-pathologic correlation. Biomed J 45:38–49. https://doi.org/10.1016/j.bj.2021.08.009
3. King CR, Zhang A, Mymryk JS. 2016. The persistent mystery of adenovirus persistence. Trends Microbiol 24:323–324. https://doi.org/10.1016/j.tim.2016.02.007
4. Jin Y, Zhang R, Xie Z, Yan K, Gao H, Song J, Yuan X, Hou Y, Duan Z. 2013. Prevalence of adenovirus in children with acute respiratory tract infection in Lanzhou, China. Virol J 10:271. https://doi.org/10.1186/1743-422X-10-271
5. Lee WJ, Jung HD, Cheong HM, Kim K. 2015. Molecular epidemiology of a post-influenza pandemic outbreak of acute respiratory infections in Korea caused by human adenovirus type 3. J Med Virol 87:10–17. https://doi.org/10.1002/jmv.23984
6. Ghebremedhin B. 2014. Human adenovirus: viral pathogen with increasing importance. Eur J Microbiol Immunol (Bp) 4:26–33. https://doi.org/10.1556/EuJMI.4.2014.1.2
7. DeRN, Van DerPC, Brenkman AB. 2003. Adenovirus DNA replication: protein priming, jumping back and the role of the DNA binding protein DBP. Adenoviruses: model and vectors in virus-host interactions 272:187–211. https://doi.org/10.1007/978-3-662-05597-7_7
8. Pelka P, Ablack JNG, Fonseca GJ, Yousef AF, Mymryk JS. 2008. Intrinsic structural disorder in adenovirus E1A: a viral molecular hub linking multiple diverse processes. J Virol 82:7252–7263. https://doi.org/10.1128/JVI.00104-08
9. Radko S, Koleva M, James KMD, Jung R, Mymryk JS, Pelka P. 2014. Adenovirus E1A targets the DREF nuclear factor to regulate virus gene expression, DNA replication, and growth. J Virol 88:13469–13481. https://doi.org/10.1128/JVI.02538-14
10. Pickart CM, Eddins MJ. 2004. Ubiquitin: structures, functions, mechanisms. Biochimica et Biophysica Acta (BBA) - Molecular Cell Research 1695:55–72. https://doi.org/10.1016/j.bbamcr.2004.09.019
11. Welcker M, Larimore EA, Frappier L, Clurman BE. 2011. Nucleolar targeting of the Fbw7 ubiquitin ligase by a pseudosubstrate and glycogen synthase kinase 3. Mol Cell Biol 31:1214–1224. https://doi.org/10.1128/MCB.01347-10
12. Davis ME, Gack MU. 2015. Ubiquitination in the antiviral immune response. Virology 479–480:52–65. https://doi.org/10.1016/j.virol.2015.02.033
13. Akira S. 2013. Pathogen recognition receptors and innate immunity. Xenotransplantation 20:351–351. https://doi.org/10.1111/xen.12060_17
14. Bauer M, Flatt JW, Seiler D, Cardel B, Emmenlauer M, Boucke K, Suomalainen M, Hemmi S, Greber UF. 2019. The E3 ubiquitin ligase mind bomb 1 controls adenovirus genome release at the nuclear pore complex. Cell Rep 29:3785–3795. https://doi.org/10.1016/j.celrep.2019.11.064

15. Rajsbaum R, García-Sastre A, Versteeg GA. 2014. Trimmunity: the roles of the TRIM E3-ubiquitin ligase family in innate antiviral immunity. J Mol Biol 426:1265–1284. https://doi.org/10.1016/j.jmb.2013.12.005
16. Kawai T, Akira S. 2006. Innate immune recognition of viral infection. Nat Immunol 7:131–137. https://doi.org/10.1038/ni1303
17. van Gent M, Sparrer KMJ, Gack MU. 2018. TRIM proteins and their roles in antiviral host defenses. Annu Rev Virol 5:385–405. https://doi.org/10.1146/annurev-virology-092917-043323
18. Fu B, Wang L, Ding H, Schwamborn JC, Li S, Dorf ME, Basler CF. 2015. TRIM32 senses and restricts influenza A virus by ubiquitination of PB1 polymerase. PLoS Pathog 11:e1004960. https://doi.org/10.1371/journal.ppat.1004960
19. Bagga T, Tulsian NK, Mok YK, Kini RM, Sivaraman J. 2022. Mapping of molecular interactions between human E3 ligase TRIM69 and dengue virus NS3 protease using hydrogen-deuterium exchange mass spectrometry. Cell Mol Life Sci 79:233. https://doi.org/10.1007/s00018-022-04245-x
20. Patil G, Zhao M, Song K, Hao W, Bouchereau D, Wang L, Li S. 2018. TRIM41-mediated ubiquitination of nucleoprotein limits influenza A virus infection. J Virol 92:e00905-18. https://doi.org/10.1128/JVI.00905-18
21. Di Pietro A, Kajaste-Rudnitski A, Oteiza A, Nicora L, Towers GJ, Mechti N, Vicenzi E. 2013. TRIM22 inhibits influenza A virus infection by targeting the viral nucleoprotein for degradation. J Virol 87:4523–4533. https://doi.org/10.1128/JVI.02548-12
22. Chen Z, Wang Z, Guo W, Zhang Z, Zhao F, Zhao Y, Jia D, Ding J, Wang H, Yao M, He X. 2015. TRIM35 interacts with pyruvate kinase Isoform M2 to suppress the warburg effect and tumorigenicity in hepatocellular carcinoma. Oncogene 34:3946–3956. https://doi.org/10.1038/onc.2014.325
23. Sun N, Jiang L, Ye M, Wang Y, Wang G, Wan X, Zhao Y, Wen X, Liang L, Ma S, Liu L, Bu Z, Chen H, Li C. 2020. TRIM35 mediates protection against influenza infection by activating TRAF3 and degrading viral PB2. Protein Cell 11:894–914. https://doi.org/10.1007/s13238-020-00734-6
24. Luo W, Zhang J, Liang L, Wang G, Li Q, Zhu P, Zhou Y, Li J, Zhao Y, Sun N, Huang S, Zhou C, Chang Y, Cui P, Chen P, Jiang Y, Deng G, Bu Z, Li C, Jiang L, Chen H, Perez DR. 2018. Phospholipid scramblase 1 interacts with influenza A virus NP, impairing its nuclear import and thereby suppressing virus replication. PLoS Pathog 14:e1006851. https://doi.org/10.1371/journal.ppat.1006851
25. Costa R, Akkerman N, Graves D, Crisostomo L, Bachus S, Pelka P. 2020. Characterization of adenovirus 5 E1A Exon 1 deletion mutants in the viral replicative cycle. Viruses 12:213. https://doi.org/10.3390/v12020213
26. Finley D. 2009. Recognition and processing of ubiquitin-protein conjugates by the proteasome. Annu Rev Biochem 78:477–513. https://doi.org/10.1146/annurev.biochem.78.081507.101607
27. Zhong B, Zhang Y, Tan B, Liu TT, Wang YY, Shu HB. 2010. The E3 ubiquitin ligase Rnf5 targets virus-induced signaling adaptor for ubiquitination and degradation. The Journal of Immunology 184:6249–6255. https://doi.org/10.4049/jimmunol.0903748
28. Zhang Y, Zhang H, Zheng G-L, Yang Q, Yu S, Wang J, Li S, Li L-F, Qiu H-J, López S. 2019. Porcine RING finger protein 114 inhibits classical swine fever virus replication via K27-linked polyubiquitination of viral Ns4B. J Virol 93. https://doi.org/10.1128/JVI.01248-19
29. Joazeiro CAP, Weissman AM. 2000. RING finger proteins: mediators of ubiquitin ligase activity. Cell 102:549–552. https://doi.org/10.1016/s0092-8674(00)00077-5
30. Berndsen CE, Wolberger C. 2014. New insights into ubiquitin E3 ligase mechanism. Nat Struct Mol Biol 21:301–307. https://doi.org/10.1038/nsmb.2780
31. Kueck T, Bloyet LM, Cassella E, Zang T, Schmidt F, Brusic V, Tekes G, Pornillos O, Whelan SPJ, Bieniasz PD. 2019. Vesicular Stomatitis virus transcription is inhibited by TRIM69 in the interferon-induced antiviral state. J Virol 93:e01372-19. https://doi.org/10.1128/JVI.01372-19
32. Li Y, Wu H, Wu W, Zhuo W, Liu WX, Zhang YX, Cheng MZ, Chen YG, Gao N, Yu HT, Wang LF, Li W, Yang MJ. 2014. Structural insights into the TRIM family of ubiquitin E3 ligases. Cell Res. 24:762–765. https://doi.org/10.1038/cr.2014.46
33. Liu BY, Zhang M, Chu HL, Zhang HH, Wu HF, Song GH, Wang P, Zhao K, Hou JX, Wang X, Zhang L, Gao CJ. 2017. The ubiquitin E3 ligase TRIM31 promotes aggregation and activation of the signaling adaptor MAVS through Lys63-linked Polyubiquitination. Nat Immunol 18:214–224. https://doi.org/10.1038/ni.3641
34. Grumati P, Dikic I. 2018. Ubiquitin signaling and autophagy. J Biol Chem 293:5404–5413. https://doi.org/10.1074/jbc.TM117.000117
35. Cohen MJ, King CR, Dikeakos JD, Mymryk JS. 2014. Functional analysis of the C-terminal region of human adenovirus E1A reveals a misidentified nuclear localization signal. Virology 468–470:238–243. https://doi.org/10.1016/j.virol.2014.08.014
36. Madison DL, Yaciuk P, Kwok RPS, Lundblad JR. 2002. Acetylation of the adenovirus-transforming protein E1A determines nuclear localization by disrupting association with importin-alpha. J Biol Chem 277:38755–38763. https://doi.org/10.1074/jbc.M207512200
37. Vragniau C, Hübner J-M, Beidler P, Gil S, Saydaminova K, Lu Z-Z, Yumul R, Wang H, Richter M, Sova P, Drescher C, Fender P, Lieber A. 2017. Studies on the interaction of tumor-derived HD5 alpha Defensins with Adenoviruses and implications for Oncolytic adenovirus therapy. J Virol 91:e02030-16. https://doi.org/10.1128/JVI.02030-16
38. Russell SJ, Peng KW, Bell JC. 2012. Oncolytic virotherapy. Nat Biotechnol 30:658–670. https://doi.org/10.1038/nbt.2287
39. Abd-Aziz N, Poh CL. 2021. Development of oncolytic viruses for cancer therapy. Transl Res 237:98–123. https://doi.org/10.1016/j.trsl.2021.04.008
40. Goradel NH, Mohajel N, Malekshahi ZV, Jahangiri S, Najafi M, Farhood B, Mortezaee K, Negahdari B, Arashkia A. 2019. Oncolytic adenovirus: a tool for cancer therapy in combination with other therapeutic approaches. Journal Cellular Physiology 234:8636–8646. https://doi.org/10.1002/jcp.27850
41. Li S, Ou M, Wang G, Tang L. 2016. Application of conditionally replicating adenoviruses in tumor early diagnosis technology, gene-radiation therapy and chemotherapy. Appl Microbiol Biotechnol 100:8325–8335. https://doi.org/10.1007/s00253-016-7806-z
42. Halldén G, Portella G. 2012. Oncolytic virotherapy with modified adenoviruses and novel therapeutic targets. Expert Opin Ther Targets 16:945–958. https://doi.org/10.1517/14728222.2012.712962
43. Herrmann C, Dybas JM, Liddle JC, Price AM, Hayer KE, Lauman R, Purman CE, Charman M, Kim ET, Garcia BA, Weitzman MD. 2020. Adenovirus-mediated ubiquitination alters protein-RNA binding and aids viral RNA processing. Nat Microbiol 5:1217–1231. https://doi.org/10.1038/s41564-020-0750-9
44. Liu ML, Jiang LF, Cao WH, Wu JG, Chen XL. 2022. Identification of inhibitors and drug targets for human adenovirus infections. Viruses 14:959. https://doi.org/10.3390/v14050959
45. King CR, Tessier TM, Dodge MJ, Weinberg JB, Mymryk JS. 2020. Inhibition of human adenovirus replication by the importin alpha/Beta1 nuclear import inhibitor ivermectin. J Virol 94:e00710-20. https://doi.org/10.1128/JVI.00710-20
46. MacNeil KM, Dodge MJ, Evans AM, Tessier TM, Weinberg JB, Mymryk JS. 2023. Adenoviruses in medicine: innocuous pathogen, predator, or partner. Trends Mol Med 29:4–19. https://doi.org/10.1016/j.molmed.2022.10.001
47. Dodge MJ, MacNeil KM, Tessier TM, Weinberg JB, Mymryk JS. 2021. Emerging antiviral therapeutics for human adenovirus infection: recent developments and novel strategies. Antiviral Res 188:105034. https://doi.org/10.1016/j.antiviral.2021.105034
48. Gack MU, Albrecht RA, Urano T, Inn K-S, Huang I-C, Carnero E, Farzan M, Inoue S, Jung JU, García-Sastre A. 2009. Influenza A virus NS1 targets the ubiquitin ligase TRIM25 to evade recognition by the host viral RNA sensor RIG-I. Cell Host & Microbe 5:439–449. https://doi.org/10.1016/j.chom.2009.04.006
49. Lin DD, Zhang M, Zhang MX, Ren YJ, Jin J, Zhao QY, Pan ZS, Wu M, Shu HB, Dong C, Zhong B. 2015. Induction of USP25 by viral infection promotes innate antiviral responses by mediating the stabilization of TRAF3 and TRAF6. Proc Natl Acad Sci U S A 112:11324–11329. https://doi.org/10.1073/pnas.1509968112
50. Song H, Liu BY, Huai WW, Yu ZX, Wang WW, Zhao J, Han LH, Jiang GS, Zhang LN, Gao CJ, Zhao W. 2016. The E3 Ubiquitin Ligase TRIM31 attenuates NLRP3 Inflammasome activation by promoting Proteasomal degradation of NLRP3. Nat Commun 7:13727. https://doi.org/10.1038/ncomms13727
51. Fan Y, Li X, Zhang L, Zong Z, Wang FW, Huang J, Zeng LH, Zhang C, Yan HY, Zhang L, Zhou FF. 2022. SUMOylation in viral replication and antiviral

defense. Advanced Science 9:2104126. https://doi.org/10.1002/advs.202104126
52. Mirzalieva O, Juncker M, Schwartzenburg J, Desai S. 2022. ISG15 and ISGylation in human diseases. Cells 11:538. https://doi.org/10.3390/cells11030538
53. Enchev RI, Schulman BA, Peter M. 2015. Protein neddylation: beyond cullin-RING ligases. Nat Rev Mol Cell Biol 16:30–44. https://doi.org/10.1038/nrm3919
54. De La Cruz-Herrera CF, Shire K, Siddiqi UZ, Frappier L. 2018. A genome-wide screen of Epstein-Barr virus proteins that modulate host SUMOylation identifies a SUMO E3 Ligase conserved in Herpesviruses. PLoS Pathog. 14:e1007176. https://doi.org/10.1371/journal.ppat.1007176
55. Dalidowska I, Gazi O, Sulejczak D, Przybylski M, Bieganowski P. 2021. Heat shock protein 90 Chaperones E1A early protein of adenovirus 5 and is essential for replication of the virus. Int J Mol Sci 22:2020. https://doi.org/10.3390/ijms22042020
56. Pelka P, Miller MS, Cecchini M, Yousef AF, Bowdish DM, Dick F, Whyte P, Mymryk JS. 2011. Adenovirus E1A directly targets the E2F/DP-1 complex. J Virol 85:8841–8851. https://doi.org/10.1128/JVI.00539-11
57. Nevins JR, Raychaudhuri P, Yee AS, Rooney RJ, Kovesdi I, Reichel R. 1988. Transactivation by the adenovirus E1A gene. Biochem. Cell Biol 66:578–583. https://doi.org/10.1139/o88-068
58. King CR, Zhang A, Tessier TM, Gameiro SF, Mymryk JS, Imperiale MJ, Garsin DA. 2018. Hacking the cell: Network intrusion and exploitation by adenovirus E1A. mBio 9:mBio https://doi.org/10.1128/mBio.00390-18
59. Frisch SM, Mymryk JS. 2002. Adenovirus-5 E1A: paradox and paradigm. Nat Rev Mol Cell Biol 3:441–452. https://doi.org/10.1038/nrm827
60. Alonso-Padilla J, Papp T, Kaján GL, Benkő M, Havenga M, Lemckert A, Harrach B, Baker AH. 2016. Development of novel adenoviral vectors to overcome challenges observed with Hadv-5-based constructs. Mol Ther 24:6–16. https://doi.org/10.1038/mt.2015.194
61. Heiber J, Hyun J, Obuchi M, Barber GN. 2009. Development of recombinant vesicular stomatitis virus for use as an oncolytic vector in cancer therapy. Cytokine 48:47. https://doi.org/10.1016/j.cyto.2009.07.130
62. Biegert GWG, Rosewell Shaw A, Suzuki M. 2021. Current development in adenoviral vectors for cancer Immunotherapy. Mol Ther Oncolytics 23:571–581. https://doi.org/10.1016/j.omto.2021.11.014
63. Zhang C, Fang L, Wang X, Yuan S, Li W, Tian W, Chen J, Zhang Q, Zhang Y, Zhang Q, Zheng J. 2022. Oncolytic adenovirus-mediated expression of Decorin facilitates CAIX-targeting CAR-T therapy against renal cell carcinoma. Mol Ther Oncolytics 24:14–25. https://doi.org/10.1016/j.omto.2021.11.018
64. Zhang W, Zhang C, Tian WP, Qin J, Chen J, Zhang Q, Fang L, Zheng JN. 2020. Efficacy of an oncolytic adenovirus driven by a chimeric promoter and armed with decorin against renal cell carcinoma. Hum Gene Ther 31:651–663. https://doi.org/10.1089/hum.2019.352
65. Yang ZR, Wang HF, Zhao J, Peng YY, Wang J, Guinn BA, Huang LQ. 2007. Recent developments in the use of adenoviruses and immunotoxins in cancer gene therapy. Cancer Gene Ther 14:599–615. https://doi.org/10.1038/sj.cgt.7701054
66. Zhang W, Chen CC, Ning JF. 2021. Combining oncolytic virus with FDA approved pharmacological agents for cancer therapy. Expert Opin Biol Ther 21:183–189. https://doi.org/10.1080/14712598.2020.1811848
67. Lock M, Korn M, Wilson J, Sena-Esteves M, Gao G. 2019. Measuring the infectious titer of recombinant adenovirus using tissue culture infection dose 50% ($TCID_{50}$) end-point dilution and quantitative polymerase chain reaction (qPCR). Cold Spring Harb Protoc . https://doi.org/10.1101/pdb.prot095562